Advection versus diffusion in Richtmyer-Meshkov mixing

Doss, Forrest William

To be published in: Physics Letters A

DOI to publisher's version: 10.1016/j.physleta.2022.127976

Advection versus Diffusion in Richtmyer-Meshkov Mixing

Forrest W. Doss

Theoretical Design Division, Los Alamos National Laboratory, New Mexico USA 87545

Abstract

The Richtmyer-Meshkov (RM) instability is one of the most severe degradation mechanisms for inertial confinement fusion (ICF), and mitigating it has been a priority for the global ICF effort. In this Letter, the instability's ability to atomically mix is linked to its background decay of residual turbulent energy. We show how recently derived inequalities from the mathematical theory of PDEs constrain the evolution. A model RM process at leading order may diffusively mix or retain imprints of its initial structures indefinitely, depending on initial conditions, and there exists a theoretical range of zero-mixing for certain values of parameters. The results may apply to other systems resembling scalar transport in decaying turbulence.

Keywords: Richtmyer-Meskov instability, Reynolds-Averaged turbulence models, Telegraph equation

1. Introduction

The Richtmyer-Meshkov instability describes the material response following the impact of a shock on a structured material interface [1, 2]. It is one of the major mechanisms by which inertial fusion (ICF) schemes experience performance degradation, mixing cold, inert shell material into what should be hot, reactive fuel regions [3, 4]. Major recent improvements in ICF performance to the highest yields yet-achieved have included considerable reductions in the perturbations seeding the Richtmyer-Meshkov instability [5].

Efforts have conventionally been put into reducing the impact of Richtmyer-Meshkov by enforcing more stringent limits on the amplitudes of seed perturbations. In this Letter, we present an analysis that suggests, counterintuitively, there may be a path to suppressing mix (by diffusion) by increasing long-wavelength perturbation content, despite that this enhances the growth rate (through advection) of the Richtmyer-Meshkov instability's coherent structures. The competition between advection and diffusion is reflected at a deep level in the moment equations for turbulent fluctuations, which provides a new and robust explanation for aligned results seen in some particular computational and analytical studies [6–9]. Leveraging new mathematical results from the analysis of PDEs, this can be shown generically for single-point ensemble-averaged moments (i.e. in the Reynolds-averaging framework). At second order in the fluid equations, there is a parameter regime where fine-scale mix is predicted to disappear entirely.

2. Model construction

To study Richtmyer-Meshkov at leading order, we will first construct our model, a 'two-equation' turbulence model [10, §3.3.4] [11, §10.5] augmented with an equation for density flux. This model will be entirely conventional, but we will walk through the steps to make our choices explicit. We begin with the Euler and continuity equations,

$$\frac{DU}{Dt} = -\frac{1}{\rho}\nabla P \quad (1) \quad , \quad \frac{D\rho}{Dt} = -\rho\nabla\cdot U, \quad (2)$$

and perform Reynolds' usual perturbation expansion $U \to u'$, $\rho \to \bar{\rho} + \rho'$, in the absence of mean pressure gradients or mean background flow. Multiplying (1) by ρ' and (2) by u' and performing ensemble averaging, the transport equation for the velocity-density correlation is

$$\frac{\partial\langle u_i'\rho'\rangle}{\partial t} + \frac{\partial\langle u_i'u_j'\rho'\rangle}{\partial x_j} = -\langle u_i'u_j'\rangle\frac{\partial\bar{\rho}}{\partial x_j} + \bar{\rho}\left\langle v'\frac{\partial P'}{\partial x_i}\right\rangle. \quad (3)$$

Meanwhile, Reynolds averaging of (2) alone yields

$$\frac{\partial\bar{\rho}}{\partial t} = -\nabla\cdot\langle u'\rho'\rangle. \tag{4}$$

Equation 4 identifies the correlation $\langle u'\rho'\rangle$ as a current density for the mean expected mass field, to which (3) serves as a constitutive equation. We make replacements to close the other moments which appeared,

$$\langle u'u'\rangle\nabla\bar{\rho} \to k\nabla\bar{\rho},\ \bar{\rho}\left\langle v'\frac{\partial P'}{\partial x_i}\right\rangle \to -C_\theta\omega\langle u'\rho'\rangle \tag{5}$$

where k represents the specific turbulent kinetic energy density of random fluctuations, ω is a turbulent turnover rate, and C_θ is a constant parameter. Any anisotropy of the energy is assumed constant and absorbed into the scale of k. The variables k and ω are assumed spatially homogenous, to have been seeded in the earlier phases of the instability, and to be self-similar in the sense that they are governed by a single complete set of length and time variables. Dimensionally, this means they may be modeled by the two-equation system [10, 11]

$$\frac{\partial k}{\partial t} = -\omega k,\ \frac{\partial\omega}{\partial t} = -\frac{\omega^2}{n}, \tag{6}$$

where n is a decay constant. We will assume everywhere that we have freely decaying turbulence with $2 > n > 0$. The solutions of (6) with initial conditions (i.c.s) $\omega(\omega_0^{-1}) = \omega_0$ and $k(\omega_0^{-1}) = k_0$ are

$$\omega = \frac{n\omega_0}{n-1+t\omega_0},\ k = k_0\left(\frac{\omega_0}{\omega}\right)^{-n}. \tag{7}$$

The second replacement in (5) expresses the pressure-density correlation as a scattering term proportional to the turbulent rate ω. This form can be motivated theoretically as a variation of Rotta's return-to-isotropy analysis [12], and C_θ (sometimes called the Monin constant [13]) is found in high Reynolds-number flows to have a typical value around 3, though it may scale with Reynolds number [14].

As a final closure, we will omit the triply-nonlinear term $\langle u'u'\rho'\rangle$. This neglects the nonlinearity of the Navier-Stokes equations as it pertains to ρ', while retaining its coupling to $\bar{\rho}$. Thus truncating (3) at second order, taking the divergence of each side, and applying continuity using (4), we obtain a mass transport equation

$$\frac{\partial^2\bar{\rho}}{\partial t^2} - k\nabla^2\bar{\rho} + C_\theta\omega\frac{\partial\bar{\rho}}{\partial t} = 0 \tag{8}$$

where k and ω are the decaying-in-time parameters of the background turbulence. Equation 8 is known as the telegraph equation. It has characteristics of both the wave equation (including a finite propagation speed of disturbances) and the heat equation (smoothing of initial structure), and appears frequently as a model for transport [15].

Our model deviates from the classical telegraph equation by the parameters' evolution in Eqs. 7, according to which the energy k goes as $\sim t^{-n}$ and the eddy rate $\omega \sim t^{-1}$. These variable coefficients have implications for the balance of wave- vs. heat-like behaviors, which can be interpreted as the relative ability of structures in $\bar{\rho}$ to advect intact as opposed to spread around through diffusion. Diffusion in the moment picture does not precisely imply uniform mixing through physical diffusion (which is not included in (2)), but represents chaotic advection of the material leading to a mixed average and, in the standard picture, to a spectral cascade to the fine scales where irreversible molecular mixing will occur [16].

3. Decaying Turbulence

We now investigate (8) and where it falls in diffusion- vs. wave-like behaviors in relation to its initial information. The effects of the decaying background turbulence according to (7) have competing impacts — an increasing 'wave speed' in $\sqrt{k}$ has an apparently diffusive effect, by spreading out initial data over increasingly more space, while decreasing 'wave speed' has the opposite effect of collapsing them closer together, and the scattering term proportional to ω has an unconditionally diffusive effect. We introduce a transformation to aggregate their combined influence. First we introduce a nondimensional time s by $s = (t\omega_0 - 1)/n$. ($s = 0$ at $t = w_0^{-1}$, when the i.c.s are defined.) In this variable,

$$\frac{\partial^2\bar{\rho}}{\partial s^2} - \frac{k_0 n^2}{\omega_0^2(1+s)^n}\nabla^2\bar{\rho} + \frac{C_\theta n}{1+s}\frac{\partial\bar{\rho}}{\partial s} = 0.$$

Next, we introduce new contracting coordinates

$$\hat{t} = \frac{2(1+s)^{1-\frac{n}{2}}}{2-n},\ \hat{x} = \frac{x}{\lambda_0},\ \lambda_0 \equiv \sqrt{\frac{k_0 n^2}{\omega_0^2}}$$

and multiply through by $(1+s)^n$ to isolate the time-dependence to the first-order term,

$$\frac{\partial^2\bar{\rho}}{\partial\hat{t}^2} + \frac{\mu}{\hat{t}}\frac{\partial\bar{\rho}}{\partial\hat{t}} - \hat{\nabla}^2\bar{\rho} = 0 \tag{9}$$

where the multiplier μ is

$$\mu \equiv \left(-\frac{n}{2-n}+\frac{2C_\theta n}{2-n}\right)=\frac{n(2C_\theta-1)}{2-n}. \qquad (9')$$

The decay constant n and the scattering constant C_θ together completely parameterize the system's evolution through μ.

In Equation 9 we have rearranged (8) into a telegraph equation with constant speed and decaying dissipation. Notice that the portion of dissipation which was evoked from the decaying wave speed (the part of (9′) which does not depend on C_θ) is *negative*. If $C_\theta < 1/2$, we have backwards diffusion unphysically enhancing concentrations and potentially blowing up. Interestingly, this bound coincides with the realizability limit for C_θ from stochastic models [12].

The final dissipation term in (9) decays away as $\sim \hat{t}^{-1}$. In the analytic theory of PDEs, it has been lately proved that when dissipation decays more rapidly than $\hat{t}^{-1}$ (called *non-effective* dissipation), (9) has all of the structure-preserving properties of the wave equation. Slower than $\hat{t}^{-1}$ (*effective* dissipation), it has the smoothing property of the heat equation. For the present case we are on the boundary, and as μ runs from 0 to ∞ the equation becomes *effective* with respect to various heat-like qualities as μ passes different thresholds [17–21]. One of these occurs at $\mu = 2$, below which all modal content in $\bar{\rho}$ dissipates equally, and above which modes dissipate faster at shorter scales, transitioning from spectral preservation (wavelike) to diffuse solutions (heatlike), and the overall time-decay of these derivatives increases with μ. By a theorem of Wirth, the result is function-analytically expressed in terms of so-called energy norms as $\mathbb{E} \sim \mathcal{O}(\hat{t}^{-\min(\mu,2)})$, where $\mathbb{E} = \langle(\partial_{\hat{t}}\bar{\rho})^2 + (\hat{\nabla}\bar{\rho})^2\rangle$ and $\langle\,\rangle$ denotes an integration over $\hat{x}$ [19, Thm. 3.4].

Below $\mu = 1$, a related result holds for an amplitude-norm $\mathbb{S}$ rather than for derivatives. Interpreting the modal content in $\bar{\rho}$ as fluctuations around an asymptotic state $\bar{\rho}(x,t) = \rho_0 + \rho'(x,t)$, the result can be expressed as bounds on the density variance $\mathbb{S} = \langle\rho'^2\rangle$, that $\langle\rho'^2\rangle \lesssim \mathcal{O}(\hat{t}^{1-\min(\mu,1)})$. When $\mu < 1$, $\langle\rho'^2\rangle$ can be globally preserved or even increase (i.e. the *focusing* property of wave equations is possible) while when $\mu > 1$, $\langle\rho'^2\rangle$ can only remain constant or, more likely, decay [19, 22]. This is interesting because the ensemble-averaged $\langle\rho'^2\rangle$ is a natural measure of subscale mixedness, which decreases to 0 in the limit of atomic mix [23]. Connecting the $\langle$spatial$\rangle$ and $\langle$ensemble$\rangle$ averages in-

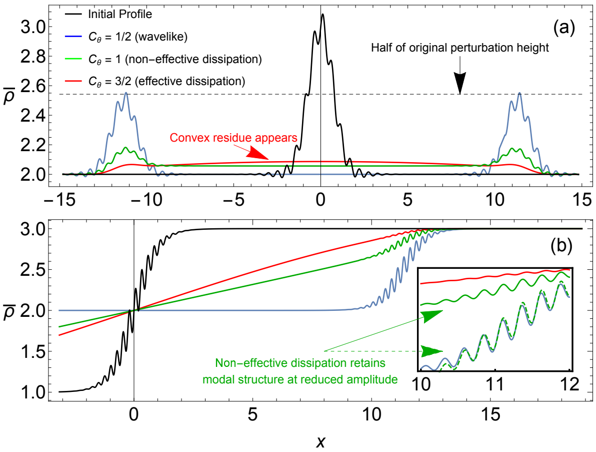

Figure 1: Representative cases of (a) diffusing local concentration, $\bar{\rho}(\omega_0^{-1}) = 2 + \exp(-x^2) + 0.1\sin(12x)\exp(-x^2/4)$, and (b) diffusing initial density interface, $\bar{\rho}(\omega_0^{-1}) = 2 + \tanh(x) + .2\sin(24x)\exp(-x^2)$, at $t = 70$. $k_0 = 1, \omega_0 = 1$, $n = 1.3$. Black — initial conditions. Blue — $C_\theta = 1/2$ (wave-like, $\mu = 0$), Green — $C_\theta = 1$ (non-effective, $\mu \approx 1.86$), Red — $C_\theta = 1.5$ (effective, $\mu \approx 3.7$).

vokes a somewhat imprecise (but not uncommon) ergodic hypothesis for the turbulence [24], arguing that ensemble- and spatial-fluctuations may be related. Doing so leads us to conjecture there are regimes of turbulent transport which preserve, or eliminate, density variance, separated by the critical value $\mu_c = 1$.

As the mathematics are somewhat abstract, Figure 1 shows some example numerical solutions of (8) for 1D profiles, illustrating changes of behavior with μ. To keep the horizontal scale comparable between cases, n is fixed and C_θ is varied. In 1a, we show dispersion of a local concentration maximum, with some asymmetric high-mode structure superimposed. The blue curve ($\mu = 0$) is wave-like – the solution is two half-height copies of the i.c.s propagating in opposite directions. The green solution ($\mu < 2$) shows the same structure as the blue solution, but decayed in overall amplitude, while the red solution ($\mu > 2$) has smoothed the i.c.s, retaining only a weak imprint. Notice also the appearance of an excess around the origin when $\mu > 2$, as long wavelengths begin to preferentially survive.

Below that, in Figure 1b, we illustrate the dispersion of an initially nearly-sharp density interface, again with high-mode structure. The solution is symmetric in an obvious way, so we provide an inset in which differences are more clearly observed. Again, the wave-like (blue) curve is propagating outward. The inset (dashed curve) shows the non-effective (green) solution amplified by $3\times$ and shifted to overlay the blue, highlighting the conserved modal structure. The diffusive (red) curve shows the surviving structure being confined further from the center and closer to the front as time progresses. These examples differentiate propagation of structure with increasing μ in two canonical cases, the latter of which is a prototype for the Richtmyer-Meshkov instability geometry.

4. The Richtmyer-Meshkov Instability

So far everything we have discussed is equally applicable to transport in any decaying turbulence field, not just Richtmyer-Meshkov. We will now apply the theory to what may be considered a special, particularly complex case of transport in a decaying turbulent field. The energy for the turbulence in the Richtmyer-Meshkov instability comes from a shock crossing a structured interface. The shock excites unstable modes on the interface, which rapidly evolve to nonlinearity and subsequently to developed, mixing flow. It is often viewed as the 'impulsive counterpart' of the continuously driven Rayleigh-Taylor instability [1, 25, 26]. In this line of thinking, which approximates away the details of the shock and reflected waves, after the passing of the impulsive acceleration the fluid densities cease to be hydrodynamically relevant.

While this is most appropriate when both shocks and density contrast are mild, complexities will still arise due to the Richtmyer-Meshkov instability's shock-driven nature. Energy is deposited into the velocity field at distances proportional to the longest wavelengths in the interface, and so at scales local to the interface itself may appear homogeneous [27, 28]. The velocity field retains information about the spectral content of the surface in its long-range correlations, opening the possibility for non-standard energy decay rates [29–31]. The resulting turbulence can be initially strongly aligned in the shock direction and retain this anisotropy, and it remains not fully understood with what rates or conditions these deformations eventually relax entirely to those of free decay [32].

Nevertheless, it is generally acknowledged that after the initial shock event the flow generated by the instability is 'not fundamentally different' from decaying turbulence [27, 33], and by opening our model for decaying turbulence to non-classical decay rates we are able to describe key aspects. The model we constructed above is necessarily simple, as required to apply Wirth's theorem, but its features reflect the common fundamentals of several more sophisticated approaches [34–38]. For an up-to-date introduction to connections between this instability, statistical models, and applications, comprehensive reviews are available [39, 40].

In spite of its relative simplicity, we can show that the three-equation (for energy, time scale, and flux) model above does contain solutions which can characterize post-energy-deposition Richtmyer-Meshkov transport. Equation 9 admits a similarity solution with the desired characteristics. Letting $\mathfrak{X} = (\hat{x} + \hat{t})/(2\hat{t})$ and $u(\mathfrak{X})$ be a normalization of the density difference, (9) is reduced to the ODE

$$\left(1 - \frac{\mu}{2}\right) \frac{\partial u}{\partial \mathfrak{X}} + \frac{\mathfrak{X} - \mathfrak{X}^2}{1 - 2\mathfrak{X}} \frac{\partial^2 u}{\partial \mathfrak{X}^2} = 0. \qquad (10)$$

Since u does not appear by itself, this is amenable to a reduction of order, introducing $v = u'$. Eq. 10 can be then be separated and integrated,

$$\int \frac{\mathrm{d}v}{v} = \left(\frac{\mu}{2} - 1\right) \int \frac{1 - 2\mathfrak{X}}{\mathfrak{X} - \mathfrak{X}^2} \, \mathrm{d}\mathfrak{X},$$

yielding

$$v = ((1 - \mathfrak{X})\mathfrak{X})^{\frac{\mu}{2} - 1} \times \text{const.}$$

The similarity solution is then

$$u \propto \int ((1 - \mathfrak{X})\mathfrak{X})^{\frac{\mu}{2} - 1} \, \mathrm{d}\mathfrak{X} = I_{\mathfrak{X}}(\tfrac{\mu}{2}, \tfrac{\mu}{2}). \qquad (11)$$

In the last step, this integral was recognized as a representation of the incomplete beta function [41, Eq. 6.6.1], and the constants of integration chosen such that u runs from 0 at $\mathfrak{X} = 0$ to 1 at $\mathfrak{X} = 1$.

In physical units,

$$\mathfrak{X} = \frac{1}{2} + \frac{(2 - n)}{4} \frac{x\omega_0}{\sqrt{k_0}} \left(\frac{t\omega_0 + n - 1}{n}\right)^{\frac{n}{2} - 1}, \qquad (12)$$

so that $\mathfrak{X} = 0, 1$ correspond to physical fronts at $x(t - t_0)^{\frac{n}{2} - 1} = \text{const.}$, or propagating as $\pm x \sim (t - t_0)^{1 - \frac{n}{2}}$, where t_0 is a virtual origin.

With $\mathfrak{X}$ so defined, $\bar{\rho} = \rho_0 + \delta\rho I_{\mathfrak{X}}(\frac{\mu}{2}, \frac{\mu}{2})$ is a solution of (8), which may be patched to constant ρs matching the boundary conditions. Figure 2 shows an example solution of this form, exhibiting a spreading mixing layer. While the model is

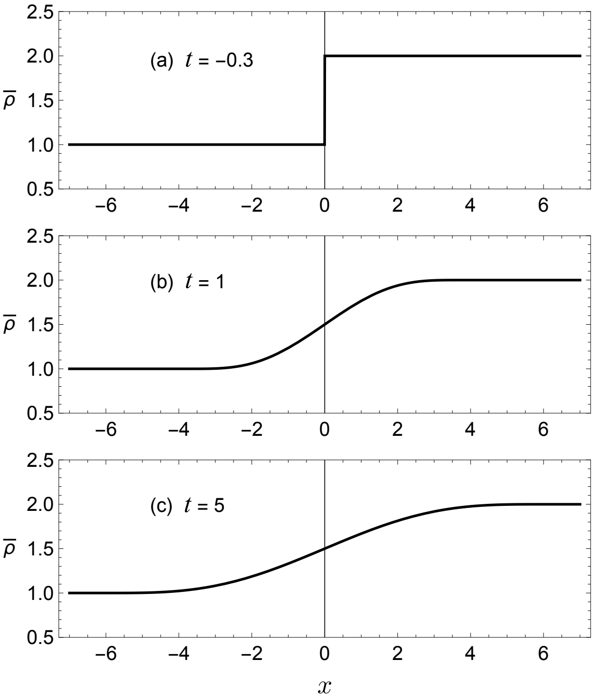

Figure 2: Solutions to (8) based on (11) and (12), with $n = 1.3, C_\theta = 2.5, \omega_0 = 1, k_0 = 1$, low density $\rho_0 = 1$, and high density $(\rho_0 + \delta\rho) = 2$. Times are given in the figures. At an earlier time (a), the solution is compatible with having originated from a sharp interface. At times $t = 1$ (b), 5 (c), and 25 (not pictured) $\mathfrak{X} = 0, 1$ correspond to $x \approx \pm 3.71$, 6.07, and 10.5 respectively, confirming $x \sim \pm(t + 0.3)^{.35}$.

technically initialized at $t\omega_0 = 1$, we can formally run the solution backwards to $t\omega_0 = (1 - n)$ where it is an initially sharp interface. The curvature of the roll-over is controlled by μ, becoming a straight line when $\mu = 2$. We cannot, however, directly observe the decoherence of structure with increasing μ as in Figure 1, since, as a similarity solution, it contains no other scales to preserve or decay. The mixing width L between pure material regions is then observed from (12) to scale as

$$L \sim (t - t_0)^\theta, \ \theta = 1 - \frac{n}{2}. \tag{13}$$

If we construct a length scale $L = \sqrt{k}/\omega$ out of our turbulence variables in (7), it will also evolve with this scaling [42–44]. Equation 13 is broadly supported by simulations of Richtmyer-Meshkov instabilities which measure it, though lack of true self-similarity produces scatter [6, 7, 45]. If we rewrite ($9'$) using (13), we find $\mu = (2C_\theta - 1)(1 - \theta)/\theta$.

Dimonte et al. [46] showed that for a prototypical interface structured by a population of modes of many wavelengths with approximately equal amplitudes, the shock interaction should have a transient phase with $\theta \approx 1/2$. Youngs and others generalized this result to suggest that effectively any $0 < \theta < 1$ could be theoretically obtained by appropriate control of the interface spectrum (a comprehensive family of proposed mechanisms for this can be found in Table I of [8], and especially those of [6, 47] are relevant here). Calculations have apparently supported this, and observed an associated transient reduction of n below 1 [7]. If n is sufficiently suppressed by an interface imposing a high θ, then there is significant room for the instability-driven transport to occur in the wave-like regime, even for high values of C_θ. We can identify a critical growth rate θ_c above which mixing should be suppressed; for $\mu_c = 1$ and $C_\theta \approx 3$, $\theta_c \approx 5/6$.

When $\mu > \mu_c$ and the instability is *effectively* mxing, we would like to predict mixedness as a function of the diffusion parameter μ. The segregation ratio Ξ (sometimes Θ) $= \int \langle c_1 c_2 \rangle \,\mathrm{d}x / \int \langle c_1 \rangle \langle c_2 \rangle \,\mathrm{d}x$, where c_i is the concentration of either of the two mixing species, is a common metric for the mix state following a Richtmyer-Meshkov instability [48]. It runs from 0 (separated) to 1 (homogeneously mixed). At the so-called buoyancy-drag-equation level, the implied mix of our μ-model is

$$\Xi(\mu) = 1 - \frac{\mu_c}{\mu} = \frac{2C_\theta - 1 - (2C_\theta - 1 + \mu_c)\theta}{(2C_\theta - 1)(1 - \theta)}, \tag{14}$$

with $\mu_c = 1$ conjectured. Buoyancy-drag modeling operates more coarsely than Reynolds-averaging, recasting (3) and (6) as a single equation for the turbulent self-similar length scale. It is useful here because it unifies several properties of Richtmyer-Meshkov with transients of the Rayleigh-Taylor instability [49–55]. Previous work suggests a closure of the form $B = (1 - \Xi)(1 - \theta)/\theta$, with B a parameter [54, see also 55, Eqs. 51-53]. Solving for Ξ using ($9'$) & (13), and setting B by enforcing $\Xi = 0$ at $\mu = \mu_c$, we get (14). This automatically satisfies $\Xi \to 1$ as $\mu \to \infty$.

Fig. 3 summarizes our $\Xi(\mu)$ against results from the literature and predictions of mix (Ξ_2) of a spectral model based on permanence of certain invariants [8]

$$\Xi_2(\theta) = \frac{2 - 3\theta}{2 + (n - 3)\theta}, \ \left(\theta \leq \frac{2}{3}\right). \tag{15}$$

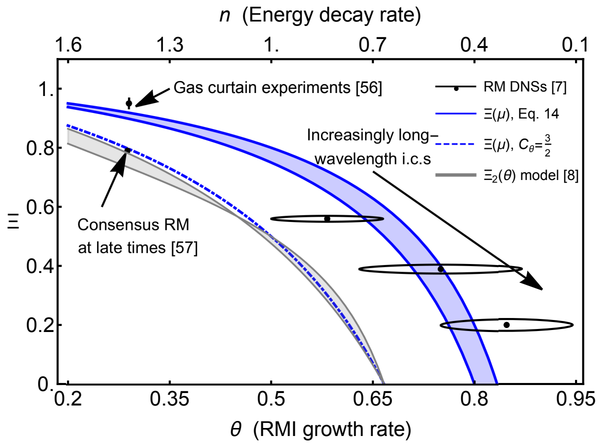

Figure 3: Black points: Calculations of mix metric Ξ against θ and n, illustrating the trend of reducing mix with increasing long wavelengths [7, 56, 57]. Ellipses represent scatter between observed θ and n compared with (13). Gray band: $\Xi_2(\theta)$, from [8, Eq. 36]. Blue: (shaded) $\Xi(\mu)$ from (14) for the range $C_\theta = 2.5$ (below) to 3 (above), and (dashed) $C_\theta = 3/2$.

The bands for the $\Xi_2(\theta)$ model in Fig. 3 represent a choice of closure for n, spanning closing n by (13) as done elsewhere here or by using a constant $n = 1.1$ as done in the source. The new $\Xi(\mu)$ model from (14) overestimates the late-time mixing in 'typical' Richtmyer-Meshkov (by which time our homogeneity of energy approximation is invalidated), but effectively captures post-shock simulations with tailored spectra, as well as 'gas curtain' experiments, shortly after shock strikes a heavy gas slab (n is not measured by experiment; 1.4 is used here) [56].

$\Xi_2(\theta)$ in (15) is derived assuming features of the 'final period of decay,' as viscous dissipation becomes relevant at all scales. In contrast, our present model assumes the immediate post-shock transient, not long after the saturation of the longest wavelengths and at distances not far compared to them. Despite that the two models were derived by completely different methods and assumptions, the theories agree if their free parameters are adjusted to each other's regimes. In (15), θ and n are independent, while above we closed those with self-similarity via (13). If we set $n = 1$ in (15), we enforce self similarity in the 'final period' by making viscous terms dimensionally invariant [43]. If we then set $\mu_c = 1, C_\theta = 3/2$ (or $\mu_c = 2, C_\theta = 5/2$) in (14), the expressions agree for all θ, including the cut-off θ_c. The reduced C_θ compensates for energy inhomogeneity appearing over long scales and relatively late times. Also, at late times the erosion of mean gradients of density will increase the relative importance of the triply nonlinear term we neglected in (8), which may impact model validity.

For future work, on the mathematics front identifying the criteria for the heat-like transitions in more general PDEs is an ongoing area of research [for example, 58–60]. It may be possible to formally extend this analysis to *e.g.* time-varying decay n, or space-varying k, to better model late times. Nevertheless the trend in mix appears dominated by the reduction at second order modeled above.

5. Conclusions

Above, it was shown that recent results from the mathematical analysis of PDEs imply that transport of mass in a decaying turbulent field is, at the second-order, Reynolds-averaged level, of a particular critical class balanced between wave-like advection and heat-like diffusion. It was further shown that flow parameters typical of the Richtmyer-Meshkov scenario can bring the system close to critical points suggested by theory, with major effects on the amount of implied fine-scale mixing, and even suggesting an obtainable regime where mix is absent. This suggests that the different impacts of Richtmyer-Meshkov on ICF, i.e. fine-scale mix introducing cooling (dominant when $\mu > 1$) vs. gross deformation of the interfaces reducing compression (when $\mu < 1$), could be intentionally traded off through tailoring of surface spectra. This could be applied to pursue considerable practical reductions of mix in ICF.

Finally, we recall that the preceding analysis above, at its core, calls attention to an unexpected property of a scalar model for the Richtmyer-Meshkov instability, implying the conservation of structure in particular parameter regimes. The theorem identifying this property was applied in §3, before the specialization of the parameters to the instability case in §4. Because the Richtmyer-Meshkov mixing can be initialized with unusual correlations (with long ranges synchronized by the initial shock), it can naturally have decay rates n occurring around the critical points of the theory. The core result should, however, be applicable to other scenarios. For instance, resolved simulations of turbulent scalar transport with varying initial long-range spectra, which should already be described by the model as presented, may present an interesting avenue for exploring the implied suppression of mixing and its mechanism.

Acknowledgments

This work was supported by the U.S. Department of Energy and Los Alamos National Laboratory operating under contract 89233218CNA000001 with Triad National Security LLC. The author thanks the Pulsed Power Sciences Center at the Sandia National Laboratories for their hospitality, and the anonymous referees whose comments helped improve the manuscript. LA-UR-21-28236

References

[1] R. D. Richtmyer, Taylor instability in shock acceleration of compressible fluids, Communications on Pure and Applied Mathematics 12 (1960) 297.

[2] Y. Zhou, Rayleigh–Taylor and Richtmyer–Meshkov instability induced flow, turbulence, and mixing. I, Physics Reports 720-722 (2017). II, Physics Reports 723-725 (2017).

[3] T. M. *et al.*, Onset of hydrodynamic mix in high-velocity, highly compressed inertial confinement fusion implosions, Physical Review Letters 111 (2013) 085004. doi:10.1103/PhysRevLett.111.085004.

[4] V. A. Smalyuk, et al., Review of hydrodynamic instability experiments in inertially confined fusion implosions on National Ignition Facility, Plasma Physics and Controlled Fusion 62 (2020) 014007.

[5] A. B. Zylstra, et al., Hot-spot mix in large-scale HDC implosions at NIF, Physics of Plasmas 27 (2020) 092709. doi:10.1063/5.0003779, Record energetics for an inertial fusion implosion at NIF, Physical Review Letters 126 (2021) 025001. doi:10.1103/PhysRevLett.126.025001.

[6] B. Thornber, D. Drikakis, D. L. Youngs, R. J. R. Williams, The influence of initial conditions on turbulent mixing due to Richtmyer–Meshkov instability, Journal of Fluid Mechanics 654 (2010) 99.

[7] M. Groom, B. Thornber, The influence of initial perturbation power spectra on the growth of a turbulent mixing layer induced by Richtmyer–Meshkov instability, Physica D 407 (2020) 132463.

[8] O. Soulard, F. Guillois, J. Griffond, V. Sabelnikov, S. Simoëns, Permanence of large eddies in Richtmyer-Meshkov turbulence with a small Atwood number, Physical Review Fluids 3 (2018) 104603.

[9] Y. Zhou, M. Groom, B. Thornber, Dependence of enstrophy transport and mixed mass on dimensionality an initial conditions in the Richtmyer-Meshkov instability induced flows, Journal of Fluids Engineering 142 (2020) 121104.

[10] W. D. McComb, The Physics of Fluid Turbulence, Oxford University Press, 1990.

[11] S. P. Pope, Turbulent Flows, Cambridge University Press, 2000.

[12] P. Durbin, Y. Shabany, Toward consistent formulation of Reynolds stress and scalar flux closures, Fluid Dynamics Research 20 (1997) 115. doi:10.1016/S0169-5983(96)00048-2.

[13] A. S. Monin, On the symmetry properties of turbulence in the surface layer of air, Izvestiya, Atmospheric and Oceanic Physics 1 (1965) 25. Cited in [61].

[14] O. Zeman, Progress in the modeling of planetary boundary layers, Annual Review of Fluid Mechanics 13 (1981) 253.

[15] A. S. Monin, A. M. Yaglom, Statistical Fluid Mechanics, MIT Press, 1971. ,§10.6 reviews telegraph models going back to Taylor [62].

[16] G. K. Batchelor, Small-scale variation of convected quantities like temperature in turbulent fluid, Journal of Fluid Mechanics 5 (1959) 113. doi:10.1017/S002211205900009X.

[17] K. Nishihara, $L^p - L^q$ estimates of solutions to the damped wave equation in 3-dimensional space and their application, Mathematische Zeitschrift 244 (2003) 631.

[18] M. Reissig, $L_p - L_q$ decay estimates for wave equations with time-dependent coefficients, Journal of Nonlinear Mathematical Physics 11 (2004) 534.

[19] J. Wirth, Solution representations for a wave equation with weak dissipation, Mathematical Methods in the Applied Sciences 27 (2004) 101.

[20] M. D'Abbicco, The threshold of effective damping for semilinear wave equations, Mathematical Methods in the Applied Sciences 38 (2015) 1032.

[21] T. Inui, H. Mizutani, Scattering and asymptotic order for the wave equations with scale-invariant damping and mass, Nonlinear Differential Equations and Applications 28 (2021). Remarks on asymptotic order for the linear wave equation with the scale-invariant damping and mass with L^r-data, Proceedings of the American Mathematical Society 149 (2021) 3473.

[22] R. S. Strichartz, *A priori* estimates for the wave equation and some applications, Journal of Functional Analysis 5 (1970) 218.

[23] J. R. Ristorcelli, Exact statistical results for binary mixing and reaction in variable density turbulence, Physics of Fluids 29 (2017) 020705. doi:10.1063/1.4974517.

[24] B. Galanti, A. Tsinober, Is turbulence ergodic?, Physics Letters A 330 (2004) 173.

[25] Y. Yanh, Q. Zhang, D. Sharp, Small amplitude theory of Richtmyer-Meshkov instability, Physics of Fluids 6 (1994) 1856.

[26] M. Vandenboomgaerde, C. Mügler, S. Gauthier, Impulsive model for the Richtmyer-Meshkov instability, Physical Review E 58 (1998) 1874.

[27] B. Thornber, Y. Zhou, Energy transfer in the Richtmyer-Meshkov instability, Physical Review E 86 (2012) 056302.

[28] J. G. Wouchuk, F. Cobos-Campos, Kinetic energy of the rotational flow behind an isolated rippled shock wave, Physica Scripta 93 (2018) 094003.

[29] P. A. Davidson, The minimum energy decay rate in quasi-isotropic grid turbulence, Physics of Fluids 23 (2011) 085108.

[30] A. Llor, Langevin equation of big structure dynamics in turbulence: Landau's invariant in the decay of homogeneous isotropic turbulence, European Journal of Mechanics B/Fluids 30 (2011) 480.

[31] W. D. McComb, Infrared properties of the energy spectrum in freely decaying isotropic turbulence, Physical Review E 93 (2016) 013103.

[32] V. K. Tritschler, S. Hickel, X. Y. Hu, N. A. Adams, On the Kolmogorov inertial subrange developing from Richtmyer-Meshkov instability, Physics of Fluids 25 (2013) 071701.

[33] V. K. Tritschler, M. Zubel, S. Hickel, N. A. Adams, Evolution of length scales and statistics of Richtmyer-

Meshkov instability from direct numerical simulations, Physical Review E 90 (2014) 063001.

[34] O. Grégoire, D. Souffland, S. Gauthier, A second-order turbulence model for gaseous mixtures induced by Richtmyer-Meshkov instability, Journal of Turbulence 6 (2005).

[35] J. D. Schwarzkopf, D. Livescu, R. A. Gore, R. M. Rauenzahn, J. R. Ristorcelli, Application of a second-moment closure model to mixing processes involving multicomponent miscible fluids, Journal of Turbulence 12 (2011).

[36] B. E. Morgan, M. E. Wickett, Three-equation model for the self-similar growth of Rayleigh-Taylor and Richtmyer-Meshkov instabilities, Physical Review E 91 (2015) 043002.

[37] O. Schilling, Self-similar Reynolds-averaged mechanical-scalar turbulence models for Rayleigh-Taylor, Richtmyer-Meshkov, and Kelvin-Helmholtz instability-induced mixing in the small Atwood number limit, Physics of Fluids 33 (2021) 085129.

[38] N. O. Braun, R. A. Gore, A multispecies turbulence model for the mixing and de-mixing of miscible fluids, Journal of Turbulence 22 (2021) 784. doi:10.1080/14685248.2021.1983180.

[39] Y. Zhou, T. T. Clark, D. S. Clark, S. G. Glendinning, M. A. Skinner, C. M. Huntington, O. A. Hurricane, A. M. Dimits, B. A. Remington, Turbulent mixing and transition criteria of flows induced by hydrodynamic instabilities, Physics of Plasmas 26 (2019) 080901. doi:10.1063/1.5088745.

[40] Y. Zhou, R. J. R. Williams, P. Ramaprabhu, M. Groom, B. Thornber, A. Hillier, W. Mostert, B. Rollin, S. Balachandar, P. D. Powell, A. Mahalov, N. Attal, Rayleigh-Taylor and Richtmyer-Meshkov instabilities: a journey through scales, Physica D 423 (2021) 132838.

[41] M. Abramowitz, I. A. Stegun, Handbook of Mathematical Functions, U.S. Department of Commerce, 1972.

[42] Y. Zhou, A scaling analysis of turbulent flows driven by Rayleigh-Taylor and Richtmyer-Meshkov instabilities, Physics of Fluids 13 (2001).

[43] T. T. Clark, Y. Zhou, Growth rate exponents of Richtmyer-Meshkov mixing layers, Journal of Applied Mechanics 73 (2006) 461.

[44] A. Llor, Bulk turbulent transport and structure in Rayleigh-Taylor, Richtmyer-Meshkov, and variable acceleration instabilities, Laser and Particle Beams 21 (2003) 305.

[45] V. K. Tritschler, B. J. Olson, S. K. Lele, S. Hickel, X. Y. Hu, N. A. Adams, On the Richtmyer-Meshkov instability evolving from a deterministic multimode planar interface, Journal of Fluid Mechanics 755 (2014) 429.

[46] G. Dimonte, C. E. Ferking, M. Schneider, Richtmyer-Meshkov instability in the turbulent regime, Physical Review Letters 74 (1995) 4855.

[47] B. Thornber, D. Drikakis, D. L. Youngs, R. J. R. Williams, Physics of the single-shocked and reshocked Richtmyer–Meshkov instability, Journal of Turbulence 13 (2012).

[48] Y. Zhou, W. H. Cabot, B. Thornber, Asymptotic behavior of the mixed mass in Rayleigh-Taylor and Richtmyer-Meshkov instability induced flows, Physics of Plasmas 23 (2016) 052712.

[49] G. Dimonte, Spanwise homogeneous buoyancy-drag model for rayleigh–taylor mixing and experimental evaluation, Physics of Plasmas 7 (2000) 2255.

[50] S. I. Abarzhi, A. Gorobets, K. R. Sreenivasan, Rayleigh-Taylor turbulent mixing of immiscible, miscible and stratified fluids, Physics of Fluids 17 (2005) 081705. doi:10.1063/1.2009027.

[51] S. Bouquet, P. Candeboeuf, P. Pailhoriès, Analytical study of the buoyancy-drag equation, Mathematical Methods in the Applied Sciences 30 (2007) 2027.

[52] S. Bouquet, R. Conte, V. Kelsch, F. Louvet, Solutions of the buoyancy-drag equation with a time-dependent acceleration, Journal of Nonlinear Mathematical Physics 24 (2017) 3.

[53] B. Cheng, J. Glimm, D. H. Sharp, Density dependence of Rayleigh-Taylor and Richtmyer-Meshkov fronts, Physics Letters A 268 (2000) 366. The αs and θs in Rayleigh-Taylor and Richtmyer-Meshkov instabilities, Physica D 404 (2020) 132356.

[54] O. Poujade, M. Peybernes, Growth rate of Rayleigh-Taylor turbulent mixing layers with the foliation approach, Physical Review E 81 (2010) 016316.

[55] B.-J. Gréa, The rapid acceleration model and the growth rate of a turbulent mixing zone induced by Rayleigh-Taylor instability, Physics of Fluids 25 (2013) 015118.

[56] G. C. Orlicz, S. Balasubramanian, K. P. Prestridge, Incident shock Mach number effects on Richtmyer-Meshkov mixing in a heavy gas layer, Physics of Fluids 25 (2013) 114101. doi:10.1063/1.4827435.

[57] B. Thornber, J. Griffond, O. Poujade, N. Attal, H. Varshochi, P. Bigdelou, P. Ramaprabhu, B. Olson, J. Greenough, Y. Zhou, O. Schilling, K. A. Garside, R. J. R. Williams, C. A. Batha, P. A. Kuchugov, M. E. Ladonkina, V. F. Tishkin, N. V. Zmitrenko, V. B. Rozanov, D. L. Youngs, Late-time growth rate, mixing, and anisotropy in the multimode narrowband Richtmyer–Meshkov instability: The θ-group collaboration, Physics of Fluids 29 (2017) 105107.

[58] M. D'Abbicco, M. R. Ebert, A class of dissipative wave equations with time-dependent speed and damping, Journal of Mathematical Analysis and Applications 399 (2013) 315.

[59] M. Taylor, The diffusion phenomenon for damped wave equations with space-time dependent coefficients, Discrete and Continuous Dynamical Systems 38 (2018) 5921.

[60] M. Ikeda, T. Inuni, M. Okamoto, Y. Wakasugi, $L^p - L^q$ estimates for the damped wave equation and the critical exponent for the nonlinear problem with slowly decaying data, Communications on Pure and Applied Analysis 18 (2019) 1967. doi:10.3934/cpaa.2019090.

[61] S. B. Pope, On the relationship between stochastic Lagrangian models of turbulence and second-moment closures, Physics of Fluids 6 (1994) 973. doi:10.1063/1.868329.

[62] G. I. Taylor, Diffusion by continuous movements, Proceedings of the London Mathematical Society 20 (1922) 196. doi:10.1112/plms/s2-20.1.196.